Benchmark tests of a strongly constrained semilocal functional with a long-range dispersion correction

J. G. Brandenburg, J. E. Bates, J. Sun, and J. P. Perdew

Phys. Rev. B **94**, 115144 — Published 21 September 2016

DOI: 10.1103/PhysRevB.94.115144

Benchmark tests of a strongly constrained semilocal functional with a long-range dispersion correction

J. G. Brandenburg,[1,*] J. E. Bates,[2] J. Sun,[2] and J. P. Perdew[2,3]

[1]*London Centre for Nanotechnology, University College London, 17-19 Gordon Street, London WC1H 0AH, United Kingdom.*
[2]*Department of Physics, Temple University, Philadelphia, Pennsylvania 19122, USA*
[3]*Department of Chemistry, Temple University, Philadelphia, Pennsylvania 19122, USA*

(Dated: September 6, 2016)

The strongly constrained and appropriately normed (SCAN) semilocal density functional [J. Sun, A. Ruzsinszky, J. P. Perdew *Phys. Rev. Lett.* **115**, 036402 (2015)] obeys all 17 known exact constraints for meta-generalized-gradient approximations (meta-GGA) and includes some medium range correlation effects. Long-range London dispersion interactions are still missing, but can be accounted for via an appropriate correction scheme. In this study, we combine SCAN with an efficient London dispersion correction and show that lattice energies of simple organic crystals can be improved with the applied correction by 50%. The London-dispersion corrected SCAN meta-GGA outperforms all other tested London-dispersion corrected meta-GGAs for molecular geometries. Our new method yields mean absolute deviations (MADs) for main group bond lengths that are consistently below 1 pm, rotational constants with MADs of 0.2%, and noncovalent distances with MADs below 1%. For a large database of general main group thermochemistry and kinetics ($\sim$ 800 chemical species), one of the lowest weighted mean absolute deviations for long-range corrected meta-GGA functionals is achieved. Noncovalent interactions are of average quality and especially hydrogen bonded systems seem to suffer from overestimated polarization related to the self-interaction error of SCAN. We also discuss some consequences of numerical sensitivity encountered for meta-GGAs.

PACS numbers:

I. INTRODUCTION

Kohn-Sham density functional theory (KS-DFT)[1,2] has become an irreplaceable tool for the calculation of electronic structure in chemical and physical sciences. Within KS-DFT a noninteracting system is introduced with an effective one-particle Hamiltonian, $\hat{h}_{KS}$, whose ground state density ρ is equivalent to the interacting system. The wavefunction of the auxiliary non-interacting system is an anti-symmetrized product of single-particle eigenfunctions ψ_i (KS orbitals), the solutions of a coupled set of non-linear equations

$$\hat{h}_{KS}\psi_i(\mathbf{r}) = \epsilon_i\psi_i(\mathbf{r})\,, \tag{1}$$

$$\hat{h}_{KS} = \hat{T} + \hat{V}_{ext} + \hat{V}_{Coul} + \hat{V}_{xc}\,, \tag{2}$$

with kinetic energy operator $\hat{T}$, external potential (typically describing the fixed nuclear charges) $\hat{V}_{ext}$, the mean field Coulomb (or Hartree) potential $\hat{V}_{Coul}$, and the exchange-correlation (xc) potential $\hat{V}_{xc}$.

While DFT is in principle an exact theory, in practice the exchange-correlation energy has to be approximated. Density functional approximations (DFAs) are constructed by satisfying known exact constraints, or by empirical fitting. There are three main classes of DFAs that use only the local density and other semi-locally-available information to approximate the xc energy, E_{xc}. The first is the local spin density approximation (LSDA), which is exact for the uniform electron gas.[3] LSDA is still widely used in the solid state community with recent extensions to finite temperature free energies.[4] While extended metallic systems can be described reasonably well by LSDA, typical molecular systems require inclusion of the density gradient as in the generalized gradient approximation (GGA). The most prominent GGAs are the Perdew-Burke-Enzerhof (PBE) exchange and correlation functionals[5] and the Becke exchange (B88)[6] combined with the Lee-Yang-Parr (LYP) correlation functional.[7] A natural extension to GGAs is to use higher-order derivatives of the electron density or other semilocally-available information, leading to the meta-GGA class. A typically employed variable is the KS kinetic energy density $\tau = \frac{1}{2}\sum_i |\nabla\psi_i|^2$. Popular meta-GGAs are the Tao-Perdew-Staroverov-Scuseria (TPSS) functional[8] and the Minnesota functionals M06L,[9] M11L,[10] and MN12L[11] by Truhlar and coworkers. A recently introduced empirical meta-GGA with a smoothness constraint and a VV10 long-range dispersion correction, B97M-V, was presented by Mardirossian and Head-Gordon.[12] Constraint-satisfaction based meta-GGA functionals have gained more attention in recent years[13,14]. The SCAN functional is also a meta-GGA.[15]

In contrast to the empirical design of the Minnesota functionals, SCAN was built to satisfy the 17 known exact constraints for a semilocal functional and to fit appropriate norms (but not fit any bonded systems). Because SCAN is a major step forward in constraint satisfaction, and because its enhancement factor over local exchange is quite different[15] from those of other functionals, extensive benchmarking is necessary. In particular, one must check that the dramatic improvements of SCAN over other semilocal functionals for certain systems and properties[16] are not bought at the price of an overall

deterioration for other systems and properties. SCAN has been shown to be superior to PBE for several standard molecular and solid-state test sets.[15,16] It is the first efficient functional covering intermediate-range London dispersion interactions that demonstrates simultaneous accuracy for diversely bonded systems around equilibrium. SCAN is comparable to or even more accurate than a computationally more expensive hybrid GGA.[16] However, it is still a semilocal functional which inevitably fails for systems where the long-range effects are important, such as in the self-interaction error encountered in stretched H_2^+ and long-range van der Waals interactions.

Mixing part of the semilocal exchange with nonlocal Fock exchange can reduce the self-interaction error, and is the dominant approach in quantum chemistry. These hybrid DFAs were originally introduced by Becke and are motivated by the adiabatic connection.[17] Similarly, double-hybrid DFAs use the virtual orbital space to construct an approximate correlation energy.[18,19] Hybrid and double-hybrid DFAs are more computationally demanding than semilocal functionals. While (meta-)GGAs scale as N^3, where N is the size of the orbital basis, hybrids and double-hybrids scale as N^4 and N^5, respectively. Hybrid and double hybrid variants of SCAN have recently been reported.[20]

Long-range, attractive London dispersion interactions are important for describing extended systems such as condensed hard and soft matter, larger molecular assemblies, or adsorption processes on various surfaces. For reviews or overviews on the "dispersion problem in DFT", see Refs. 21–23. In this study we show how to combine the SCAN meta-GGA with modern London dispersion corrections. While we will focus on the most efficient D3 scheme by Grimme and coworkers[24], we will also consider the VV10 nonlocal density kernel by Vydrov and Van Voorhis.[25] A related SCAN+rVV10 scheme, where rVV10 stands for a revised VV10[26], has also been developed and yields excellent accuracy for predicting properties of layered materials.[27]

Due to their computational efficiency, (meta-)GGA DFAs are heavily relied on for the computation of geometries. For other properties (e.g., band gaps of solids), more accurate results from hybrid and double hybrid DFAs[18,28] or even high level (local) coupled cluster methods are needed.[29–31] Specifically for condensed phases, geometry optimizations with a hybrid DFA using large orbital basis sets are not amenable for routine applications. In systems with local electron density, small atom-centered orbital basis sets can be employed, which makes screened hybrid functional calculations feasible.[32] However, basis set errors have to be compensated and a meta-GGA with improved equilibrium geometries is still desired.

We begin with a short methodological description in section II. Consequences of the sensitivity with respect to integration grids sometimes encountered for meta-GGAs[33,34] are discussed in section II A. Then, the D3 and VV10 London dispersion corrections are described and the recommended damping parameters are given in section II B. Section III focuses on the accuracy of the combined SCAN-D3 method and we give a broad overview on various covalent and noncovalent bonding regimes (section III A). In addition, noncovalent interaction energies and some main group thermochemistry and kinetics are analyzed in sections III B and III C.

II. METHODOLOGY

A. The SCAN meta-GGA

A general meta-GGA form for the xc energy can be written as

$$E_{xc} = \int \mathrm{d}\mathbf{r}\, f(\rho(\mathbf{r}), \gamma(\mathbf{r}), \tau(\mathbf{r}))\,, \tag{3}$$

where we define $\gamma(\mathbf{r}) = \nabla\rho(\mathbf{r}) \cdot \nabla\rho(\mathbf{r})$. SCAN improves upon previous nonempirical meta-GGAs such as TPSS and MGGA-MS[14] by satisfying more exact constraints on the xc energy and by resolving the "order of limits" problem[35] encountered for meta-GGA parametrizations of f using both of the τ-dependent variables $z = \tau^{\mathrm{vW}}/\tau$ and α, defined below, where $\tau^{\mathrm{vW}} = |\nabla\rho|^2/8\rho$ is the von Weizsäcker kinetic energy density. Instead SCAN utilizes only the τ-dependent variable $\alpha = (\tau - \tau^{\mathrm{vW}})/\tau^{\mathrm{unif}}$ to identify different density regimes such as those found in covalent ($\alpha = 0$), metallic ($\alpha \approx 1$), and weak ($\alpha >> 1$) bonds. $\tau^{\mathrm{unif}} = (3/10)(3\pi^2)^{2/3}n^{5/3}$ is the kinetic energy density of a uniform electron density. Parametrizing the functional using α, however, can lead to some numerical sensitivity in the integration of the XC potential.

Previous works have shown that meta-GGA potential energy surfaces for dispersion bound complexes can exhibit spurious oscillations using too small integration grids[34], and that reaction energies can be severely impacted by the choice of grid as well.[36] The same issue is also inherited by some molecular properties such as nuclear gradients, and hence analytic geometry optimizations are also influenced by the choice of grid. The derivative of the SCAN energy density for atoms can exhibit oscillations near $\alpha \approx 1$ due to its functional form[37], implying a more dense grid is required for accurate integration.

The numerical grids used to evaluate the DFT contributions to the energy are built by combining angular and radial grids, so we studied the impact of convergence in both grids separately. For a given angular integration grid, slow convergence of the total energy and nuclear gradient with respect to the radial integration grid was encountered. To accurately integrate the SCAN potential, a larger number of radial points are needed in TURBOMOLE compared to previous functionals such as TPSS. Using a converged radial grid, however, the convergence of the angular grid is typically much faster, and sufficiently accurate results can be obtained using grid 4 in

TURBOMOLE which is only slightly larger than the default (grid m3). We report more detailed information on the grid dependence in the supporting information[38], the conclusions of our tests being that energy differences are less sensitive to the choice of grid than nuclear gradients. Therefore, in practice a very large radial grid is only required when computing molecular properties, and not necessarily for computation of typical reaction energies which can be adequately described using a slightly augmented radial grid.

B. London dispersion interaction

A natural formalism to obtain long-range corrections from DFT is the adiabatic fluctuation dissipation theorem[39,40], from which more approximate schemes can be obtained as discussed in two recent review rticles on modern London dispersion corrections.[41,42] One such method is the VV10 nonlocal density kernel by Vydrov and Van Voorhis[25,43–45], that is parametrized using only the local density and its reduced gradient. Two parameters are needed to determine the model; the first (C) is adjusted to reproduce reference dispersion coefficients at large distances, and the second (b) is used to damp the VV10 contribution at short distances. The parameter b can be used to adjust the VV10 kernel to any semilocal DFA.[46], while C is kept at its original value.[25]

An even more efficient alternative to VV10 is the D3 scheme which is formulated from a partitioning of the molecular polarizbility tensor. The most natural fragments in a molecule are the individual atoms since, due to their spherical symmetry, only an isotropic dynamical polarizability, $\alpha(i\omega)$, has to be considered. Thus, the correlation energy between two atoms (A and B) can be expressed by the Casimir-Polder relation[47]

$$\begin{aligned} E_c^{\mathrm{AB}} =& -\frac{C_6^{AB}}{r_{AB}^6}\,, \\ C_6^{AB} =& \frac{3}{\pi}\int_0^\infty \mathrm{d}\omega\, \alpha_A\left(i\omega\right)\alpha_B\left(i\omega\right)\,. \end{aligned} \tag{4}$$

This is the leading order fluctuating-dipole–fluctuating-dipole with the typical dependence on the atomic distance r_{AB}. The most significant difference between the various dispersion correction schemes is the way in which the C_6 coefficients are estimated.[48–53] For the D3 scheme, the dynamic polarizabilities of hydrated atoms are calculated via time-dependent DFT for reference systems, and a modified Casimir-Polder integration (similar to Eq. 4) yields the atom-pair C_6^{AB} value.[24] Higher-order dipole-quadrupole pair-terms and Axilrod-Teller-Muto type[54,55] three-body terms are calculated via recursion relations and averages, respectively, from the corresponding C_6 coefficients. The importance of many-body dispersion interactions has been recently analyzed by various groups.[56–58]

In this work, the D3 scheme is always used including the three-body term. Together, the D3 contribution to the interaction energy is

$$\begin{aligned} E_{\mathrm{c}}^{(\mathrm{D3})} =& -\frac{1}{2}\sum_{n=6,8}\sum_{A,B}^{\mathrm{pairs}}\frac{C_n^{AB}}{r_{AB}^n}f_n^d(r_{AB}) \\ & -\frac{1}{6}\sum_{A,B,C}^{\mathrm{triples}}\frac{C_9^{ABC}\left(1+3\cos\theta_A\cos\theta_B\cos\theta_C\right)}{r_{ABC}^9}f_9^d(r_{ABC}) \end{aligned} \tag{5}$$

The damping functions f_n^d are introduced to combine the D3 dispersion interaction with the semilocal correlation contribution from the DFA. The three-body term depends on the atom triangle with angles $\theta_{A/B/C}$ and geometric mean distance r_{ABC}. The two-body damping ($f_{6,8}^d$) can be either used with a zero damping (one free parameter rs_6) or a rational (Becke-Johnson) damping (two free parameter a_1 and a_2).[59] Additionally, the dipole-quadrupole C_8 terms can be scaled by a parameter s_8, which improves the interpolation between various DFAs with substantially different behavior in the medium correlation regime. Comparisons of the D3 with the VV10 dispersion correction revealed very similar accuracies.[60,61] We thus expect very similar results for SCAN-D3 and SCAN-VV10. While the VV10 scheme can adjust better to unusual electronic structures with strong charge transfer character, the D3 dispersion coefficients are typically better for organic molecules with residual error in the long-range below 5%.[23] Furthermore, the three-body term is available with highly efficient analytical derivatives, which is important for large and dense systems[62] and we will therefore mainly report results for the SCAN-D3 method throughout this study.

We have trained the damping functions using the S66x8[63] benchmark set. It consists of 66 small to medium sized molecular dimers at 8 center of mass distances with coupled cluster singles, doubles and perturbative triples reference energies at the estimated single-particle basis set limit, CCSD(T)/CBS(est.).[64] This set can be simultaneously used to test noncovalent interaction energies and equilibrium distances as recognized recently by several groups.[65–67] We interpolate the potential surfaces and extract the equilibrium minimum to compare with equilibrium binding energies and equilibrium distances at the CCSD(T) level. We fit the damping parameter by minimizing the weighted absolute relative deviations from the reference ($\delta E{+}10\delta R$). For comparison purpose, we additionally report errors on the standard S66 set in the ESI.

A summary of the optimized damping parameter for the D3 scheme in both damping variants and the VV10 scheme is given in Table I. We give the relative absolute deviations from the S66x8 reference minima and compare with the M06L and TPSS meta-GGAs, the PBE GGA and its PBE0 hybrid variant. Because the SCAN functional can cover medium-range correlation to a high degree (similarly to M06L), the dipole-quadrupole term is set to zero. Typical deviations of the various methods

TABLE I: Optimized (dimensionless) damping parameter of the D3 and VV10 dispersion correction for the SCAN functional in comparison with other methods.

	SCAN	M06L	TPSS	PBE	PBE0
plain (without correction)					
δE^a / %	22.7	14.4	56.5	45.7	43.6
δR^b / %	1.2	0.5	14.5	8.1	7.3
D3 (default rational damping[59])					
s_8	[c]0	–	1.944	0.788	1.218
a_1	[d]0.538	–	0.454	0.429	0.415
a_2	5.4200	–	4.475	4.441	4.859
δE^a / %	7.7	–	5.8	7.6	10.1
δR^b / %	0.8	–	1.7	1.2	1.1
D3(0) (zero-damping[24])					
s_8	[c]0	[c]0	1.105	0.722	0.928
rs_6	[d]1.324	1.581	1.166	1.217	1.287
δE^a / %	7.3	9.2	6.3	9.4	12.9
δR^b / %	1.0	0.5	1.5	1.7	0.9
VV10 (zero-type damping[25])					
b	[d]14.0	18.9	5.0	6.4	6.0
δE^a / %	8.4	8.0	6.3	8.3	15.6
δR^b / %	0.9	0.9	1.2	1.2	0.8

[a]Mean absolute rel. deviation of the S66x8 equilibrium energies.[63]
[b]Mean absolute rel. deviation of the S66x8 equilibrium distances.[63]
[c]Value not fitted.
[d]This work.

are 5-10% for the interaction energy and 0.5-2% for the center of mass distance. SCAN-D3 yields a good compromise of 8% and 1% error for the energy and the distance, respectively. For the intrinsically very attractive Minnesota functionals, the parameter fit of the rational damping function is not stable. This double counting problem associated with the different damping functions was recently investigated in detail.[68] SCAN also covers a large amount of medium range correlation, but both damping variants can be successfully applied with very similar accuracy.

Because the rational damping avoids artificial repulsive forces, this is typically the preferred variant. We tested SCAN with both damping variants and obtained very similar results, therefore we give only the results for the recommended rational damping scheme. If not stated otherwise, the defaults mentioned here are used throughout this study.

III. RESULTS

A. Geometries

The analysis of molecular and condensed phase geometries is separated in the following way and closely follows the strategy in Refs. 66 and 69: first the covalent bond distances of different element classes are investigated (subsection III A 1), then we highlight the interplay between covalent bond distances and medium-range correlation in medium sized molecules (subsection III A 2).

1. *Bond distances*

Though the covalent bonds are mainly determined by the semilocal xc contributions from the DFA, we use the methods with London dispersion interaction, as the correction scheme should not deteriorate the covalent bonds. In order to put the results into some broader perspective, we compare with results from M06L,[9] TPSS-D3,[8], PBE-D3,[5] and PBE0-D3.[70] The M06L meta-GGA is used as the most prominent Minnesota DFA and applied without further correction as recommended by Truhlar and coworkers.[71] In the past years, Grimme and coworkers established the TPSS-D3 meta-GGA for computing reliable geometries at rather low computational cost.[72,73] PBE-D3 is included in the comparison as the most widely applied DFA in the solid state community. Recently, extremely accurate geometries computed with the dispersion corrected hybrid functional PBE0-D3 have been reported.[66] Due to the nonlocal Fock exchange, the hybrid PBE0-D3 has significantly higher computational costs compared to the other meta-GGA based methods. We report the comparison of experimental and calculated

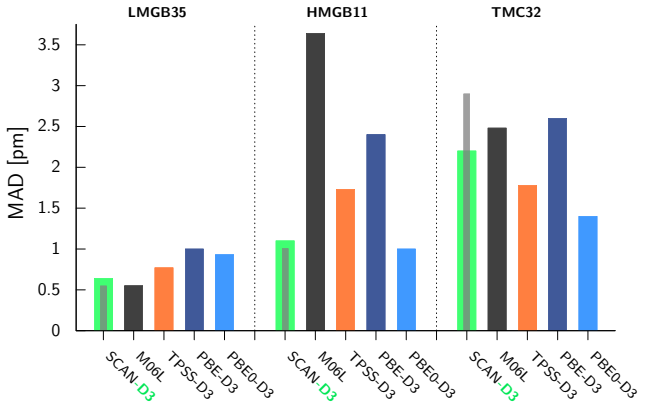

FIG. 1: Mean absolute deviations of various methods for different bond distances separated into light main group bonds (LMGB35), heavy main group bonds (HMGB11), and transition metal complexes (TMC32). For SCAN, we show both the plain functional (gray bar) and the dispersion corrected variant in order to highlight the influence of the long-range correction.

ground state equilibrium bond distances R_e (in pm) for 35 light main group bonds (LMGB35), 11 heavy main group bonds (HMGB11), and 32 3d-transition metal complexes (TMC32). The light main group bonds are sufficiently accurate with all applied methods, with mean absolute deviations (MADs) between 0.5 and 1.0 pm. Compared to the plain Hartree-Fock (HF) mean field method, which has an MAD of 2.8 pm, all semilocal DFAs lead to a substantial improvement. The base line for a good method on the HMGB11 set can be again defined by the HF MAD of 2.2 pm. While SCAN-D3 and PBE0-D3 provide excellent results with MADs slightly

below 1.0 pm, the error increases to 1.9, 2.4, and 3.6 pm for TPSS-D3, PBE-D3, and M06L, respectively. The TMC32 set of 3d-transition metal complexes is particularly interesting as its description with hybrid functionals is rather problematic.[72] This can be seen by the bad performance of HF with MAD larger than 12 pm. In contrast, meta-GGAs are the ideal choice as they do not suffer from the inclusion of HF exchange for (organo-)metallic systems and implicitly account for static correlation effects. TPSS-D3 is second only to PBE0-D3 and the 2.2 pm MAD of SCAN-D3 is very reasonable, outperforming M06L, PBE, and the uncorrected SCAN. Due to the larger systems, the impact of the dispersion interaction is significant. The error spread of SCAN-D3 drops by a factor of 2.4 when including the dispersion correction. This indicates that the D3 scheme not only leads to a systematic shift (more strongly bound systems with shorter bonds), but rather to an overall systematic improvement.

Concerning the bond lengths, the new SCAN-D3 functional provides very promising results. It clearly outperforms the PBE-D3 and TPSS-D3 functional for all main group bonds and is of similar quality for transition metal complexes. Compared to the popular M06L the bond lengths seem to be more reliable especially for heavier elements as seen in the HMGB11 benchmark set.

2. *Rotational constants*

In order to account for zero-point vibrational effects in the determination of molecular structures, gas phase rotational spectra can be measured very accurately at low temperature. From these spectra, the rotational constants, corresponding to inverse moments of inertia of the molecule, can be extracted and used to infer structural information. The accuracy of these measurements makes them an ideal benchmark observable to compare with high-level quantum-chemical calculations[74] and density functional approximations.[73,75] Very accurate, complementary theoretical predictions can help in assigning molecular conformations from rotational microwave spectroscopy.

The rotational constants of small molecules can be calculated with an MAD of only 0.04 % using well converged coupled-cluster methods.[74] For molecules with more than a few heavy atoms, this is a tremendous computational effort and it is important to have more efficient methods. A recently published set of 12 medium sized molecules has been corrected for anharmonic zero-point effects and can be directly compared to free optimizations.[76] MADs below 0.5 % were obtained with very few methods, all incorporating virtual excitations such as MP2[73], except for PBE0-D3 which is even better than MP2.[66]

In Fig. 2, the deviations of rotational constants with the reference computed with SCAN-D3 are shown alongside comparable methods. The accuracy of both SCAN and M06L meta-GGAs is excellent and exceeds the accuracy of all other tested (meta-)GGAs thus far. Since SCAN already covers medium range correlation to a high degree, the impact of the dispersion correction is smaller, but still noticeable, compared to the more repulsive TPSS or PBE0. Apparently it is possible to compute highly accurate molecular geometries using neither the virtual excitation space (dynamic correlation) nor the occupied orbital space in a nonlocal sense (Fock exchange).

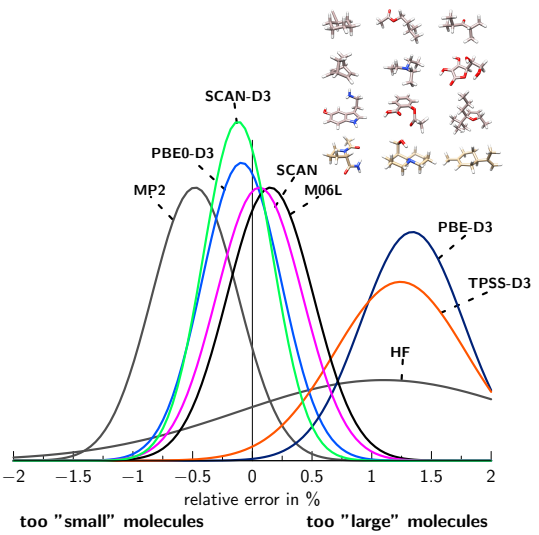

FIG. 2: Normal distribution of the relative errors in the computed rotational constants B_e for the ROT34 benchmark set with various theoretical methods. HF and MP2 results are taken from Ref. 73. The inset shows the molecules of this set.

M06L yields highly accurate geometries, but the corresponding systematic shifts are small and already indicate an overbound system with too dense molecular structures and too short noncovalent distances. In contrast, SCAN yields systematically too large molecular structures and noncovalent distances. The addition of a dispersion correction not only removes the systematic underbinding for SCAN, but also reduces the error spread on all analyzed sets except for LMGB.

B. Noncovalent interactions

As the most simple model systems for weak van der Waals interactions, we analyzed Ne_2, Ar_2, Kr_2 with the full SCAN(-D3) functional and an exchange only variant (SCANx).[77,78] Potential curves are reported in the ESI. While we see some deviations for the neon dimer, the potentials for the argon and krypton dimer are encouraging, i.e., SCANx closely reproduces the HF reference potential and SCAN-D3 is in excellent agreement with CCSD(T). More problematic is the interaction of rare gas atoms with a positive point charge, which probes the polarizability. Here, the SCAN density appears to be too polarizable with systematic deviations from the reference. This may partly explain some problems in the

description of strong hydrogen bonds discussed below.

1. Molecular dimers

We discuss two standard benchmark sets introduced by Hobza and coworkers. The first is the very well-known and widely used S22 set[79–81] comprising 22 medium-sized molecules, mostly organic complexes in their equilibrium structure. This set covers hydrogen bonded as well as typical vdW complexes and it has become the de-facto standard in the field of theoretical non-covalent interaction calculations. Significantly larger complexes are compiled in the L7 test set[82], and we use the more consistent DLPNO-CCSD(T)/CBS* interaction energies as a reference.[83]

TABLE II: Deviations of intramolecular interaction energies from the CCSD(T) references for the S22 and L7 NCI benchmark sets. (1 kcal/mol = 0.0434 eV)

measure	SCAN -D3	SCAN	M06L	TPSS -D3	PBE -D3	PBE0 -D3
S22 (binding energy in kcal/mol)[a]						
MD[b]	-0.4	0.6	0.8	0.0	-0.1	-0.3
MAD[c]	0.4	0.9	0.8	0.4	0.5	0.5
SD[d]	0.7	1.1	0.5	0.6	0.7	0.7
MAX[e]	2.6	2.9	1.7	1.5	1.9	1.8
L7 (binding energy in kcal/mol)[f]						
MD	1.2	7.9	3.0	0.9	2.1	[g]1.4
MAD	2.5	7.9	3.0	1.1	2.6	1.6
SD	3.0	5.3	2.4	1.2	2.9	1.2
MAX	4.7	15.6	6.3	2.8	6.7	3.0

[a]See Ref. 79 for details.
[b]Mean deviation, > 0 denotes underbound systems.
[c]Mean absolute deviation.
[d]Standard deviation.
[e]Maximum absolute deviation.
[f]See Refs. 82,84 for details.
[g]Values replaced by PW6B95-D3.[82]

The statistical deviations from the references are given in Table II. When comparing the different test sets, one has to keep in mind that the mean binding energies are 7.3 kcal/mol and 16.7 kcal/mol for S22 and L7, respectively.

We confirm that TPSS-D3 is one of the most accurate non-hybrid DFAs for noncovalent binding energies of molecular complexes. The MADs of 0.4 and 1.1 kcal/mol for the S22 and L7 sets are excellent, below 7% of the mean binding energy. The dispersion corrected PBE and PBE0 functionals also perform well for these sets. The plain meta-GGA M06L has substantially larger errors and the MADs are approximately double compared to TPSS-D3. While the errors could be reduced with the D3(0) scheme, this would simultaneously deteriorate the accurate geometries. Consistent with the geometry analysis, SCAN is more repulsive compared to M06L and the performance even slightly worse, especially for the L7 test set. Addition of the D3 correction significantly improves the SCAN results yielding a MAD for the L7 set of 2.5 kcal/mol (15% of the mean binding), which is still not quite as good as some of the other methods. It has been noted several times in the literature that for the highest accuracy on noncovalent energies between molecules, the D3 and related semi-classical dispersion corrections have to be combined with intrinsically more repulsive DFAs.[85,86] However, it is still notable that SCAN can profit from the dispersion correction and overall yields reasonably accurate noncovalent binding energies.

2. Molecular crystals

Molecular crystals are an increasingly important class of materials that require an accurate description from efficient methods. This is especially important for "in silico" crystal structure prediction.[87–89]

To investigate this class of systems, we analyze the X23 set of (mostly) organic molecular crystals[90,91] that can be considered as a periodic extension of S22 where the asymptotic parts of the non-covalent interaction may dominate. In order to decrease the computational effort, we compiled a subset consisting of the crystals cyclohexanedione, acetic acid, adamantane, benzene, CO_2, cyanamide, ethylcarbanate, oxalic acid, pyrazine, pyrazole, succinic acid, and uracil. The subset is constructed to maintain the MAD of TPSS-D3 for both the crystal density and the lattice energy within 0.5%.

The statistical performance is summarized in Table III and the potential energy surfaces of two selected crystals are shown in Figure 3. We show the potential energy surface (PES) of unpolar benzene, and the α polymorph of oxalic acid that contains significant hydrogen bonds. As such, the relative impact of London dispersion on the binding energy should be reduced for oxalic acid while that from electrostatic and induction effects will be more prominent. The PES of the benzene crystal in Figure 3 (a) shows again that both SCAN and M06L already cover some part of the medium range dispersion interaction. While the corresponding potentials show a clear minimum, the crystal is still underbound. The minimum of SCAN-D3 is very close to the reference after adding the D3 correction and is within "chemical accuracy" of 1 kcal/mol, similar to the TPSS-D3 and PBE0-D3 results. The equilibrium is more dense by about 3% than experimentally observed.

The oxalic acid crystal is one of the crystals within the X23 set with the strongest hydrogen bond contributions. It is therefore much more challenging for a semilocal DFA to describe the induction effects accurately as shown in Figure 3 (b). M06L is still underbound, but SCAN already computes a lattice energy close to the reference. Adding the D3 correction leads to a 4 kcal/mol overbinding with significantly too small unit cell volume. Similarly to PBE, SCAN seems to overpolarize hydrogen bond networks leading to a too attractive in-

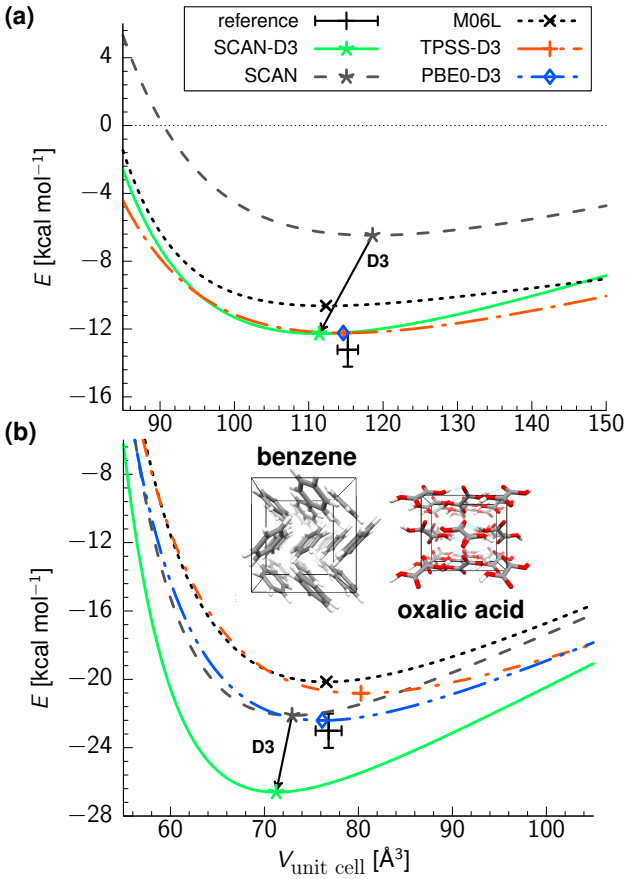

FIG. 3: Lattice energy of the (a) benzene and (b) oxalic acid α crystal based on constrained volume optimizations (TPSS-D3 level) with single-point evaluations of various dispersion corrected DFAs. For each method, the cross shows the position of the energy minimum and the arrow indicates the effect of the added dispersion correction.

duction interaction. Adding the physically correct dispersion interaction enhances the overbinding tendency, which leads to the comparably poor performance for the oxalic acid crystal. A similar effect is seen for water clusters (WATER27,[92] see below), and ice polymorphs (ICE10[93]). Another study recently reported analogous behavior for SCAN on another set of ice polymporphs.[94] TPSS-D3 has smaller errors and is even bound too weakly and as expected the best results are computed with the hybrid PBE0-D3.

Benzene and oxalic acid are two borderline cases as the other X23 systems are typically in between them as shown by the statistics given in Table III. The SCAN-D3 MAD of 4.2% for the unit cell volumes is worse compared to the uncorrected SCAN result. We attribute this mainly to the intrinsic errors of SCAN for hydrogen bonded systems. At the same time the standard deviation is slightly decreased indicating that though the D3 contribution is physically meaningful, the final SCAN-D3 method systematically underestimates the cell volumes. The geometries at the M06L level are systematically too

TABLE III: Deviations of unit cell volumes and interaction energies from the back-corrected exp. reference for the X23 organic crystal set.

measure	SCAN-D3	SCAN	M06L	TPSS-D3
	X23 (unit cell volume in %)[a]			
MD[b]	-4.2	-0.5	-3.7	1.0
MAD[c]	4.2	2.2	5.1	2.8
SD[d]	1.6	2.5	4.1	4.0
MAX[e]	6.6	4.7	8.4	15.0
	X23 (Lattice energy in kcal/mol)			
MD	1.5	-3.7	-1.2	-0.7
MAD	1.9	4.0	1.7	1.1
SD	2.0	3.2	1.7	1.1
MAX	5.0	10.5	3.4	2.2

[a]See Ref.[66,90,91] for details.
[b]Mean deviation, > 0 denotes too large distances.
[c]Mean absolute deviation.
[d]Standard deviation.
[e]Maximum absolute deviation.

dense by about 3.7% leading to an MAD larger than 5%. An additional dispersion correction would increase this systematic error even further. TPSS-D3 yielded accurate unit cell volumes with an MAD below 3%, the largest error occurring for the CO_2 crystal that is problematic for all dispersion corrected DFA methods. The SCAN-D3 lattice energies have a reasonable MAD of 1.9 kcal/mol, the dispersion correction clearly improving the performance and lowering the MAD of SCAN by more than 50%. While the performance of M06L is similar, TPSS-D3 is significantly more accurate with an MAD close to 1 kcal/mol. Other more repulsive DFAs have been shown to yield analogous, highly accurate lattice energies on this X23 set, the most successful ones being PBE0-D3, PBE0-MBD, and B86PBE-XDM.[62,90,91]

C. Thermochemistry and kinetics

In this final section we analyze the performance of the SCAN-D3 functional for general main group chemistry. In 2011, Goerigk and Grimme compiled a meta database of several benchmark sets, dubbed general main group thermochemistry, kinetics, and noncovalent interactions (GMTKN30).[28,95] It consists of three main subgroups testing basic properties (e.g., atomization energies, ionization potentials, electron and proton affinities, and reaction barriers), reaction energies (including isomerizations), and both intra and intermolecular noncovalent interactions of light and heavy molecules, including molecular conformations. This set has been extensively used to benchmark the large menagerie of DFAs from all different functional classes.[96] A transferable scheme to weight the different sets has been designed to compute an overall weighted mean absolute deviation (WTMAD), enabling a direct comparison of all methods. We compute the full GMTKN30 database with SCAN(-D3) and compare it

to the meta-GGAs M06L and TPSS-D3 and the hybrid functional PBE0-D3 in Table IV. The WTMADs of the three subgroups are shown in Figure 4.

TABLE IV: Mean absolute deviations (MAD, in kcal/mol) for all 30 subsets of the GMTKN30 database. Errors for M06L, TPSS-D3, PBE-D3 PBE0-D3 are taken from Ref. 96. For comparison, the overall WTMAD for the local spin density approximation is 11.9 kcal/mol[96].

subset	SCAN -D3	SCAN	M06L	TPSS -D3	PBE -D3	PBE0 -D3
basic properties						
MB08-165	8.1	7.9	13.3	9.5	9.2	8.6
W4-08	4.8	4.8	4.6	5.3	13.0	4.0
G21IP	4.9	4.9	4.5	4.0	3.9	3.7
G21EA	3.6	3.6	4.0	2.2	3.4	2.5
PA	3.2	3.2	4.6	4.7	2.2	2.8
SIE11	10.2	10.0	10.1	11.6	12.4	7.8
BHPERI	3.8	3.2	3.5	3.1	4.2	1.6
BH76	7.9	7.8	3.8	9.0	9.5	4.4
WTMAD (bp)	6.7	6.6	7.9	7.5	9.1	5.7
reaction energies						
BH76RC	3.7	3.7	3.1	3.7	4.4	2.5
RSE43	1.9	1.9	3.1	2.2	3.3	1.8
O3ADD6	7.4	7.1	3.4	4.4	5.0	5.7
G2RC	6.8	6.6	5.9	6.8	6.5	6.8
AL2X	2.9	2.2	1.4	2.2	2.3	1.9
NBPRC	2.9	2.4	3.9	1.7	2.3	3.3
ISO34	1.3	1.4	2.2	2.1	1.6	1.6
ISOL22	4.2	4.6	7.4	7.0	5.6	2.9
DC9	8.6	8.8	11.5	9.7	10.1	9.2
DARC	2.6	3.0	8.0	6.6	4.3	3.1
ALK6	3.8	3.4	8.1	3.3	3.6	3.6
BSR36	1.7	3.2	6.0	6.3	4.8	4.6
WTMAD (re)	2.9	3.2	4.8	4.4	4.0	3.4
non-covalent interactions						
IDISP	3.2	5.9	6.6	4.5	4.8	3.5
WATER27	9.4	7.4	2.8	4.9	8.6	6.4
S22	0.44	0.93	0.80	0.32	0.48	0.57
ADIM6	0.23	1.68	0.28	0.40	0.58	0.36
RG6	0.19	0.27	0.43	0.04	0.05	0.03
HEAVY28	0.28	0.40	0.65	0.20	0.24	0.17
PCONF	0.50	1.13	0.97	1.10	1.51	0.94
ACONF	0.16	0.32	0.46	0.05	0.09	0.10
SCONF	0.37	0.27	0.39	0.68	0.44	0.25
CYCONF	0.47	0.42	0.40	0.82	0.84	0.55
WTMAD (nci)	1.3	1.7	1.3	1.2	1.6	1.2
WTMAD (all)	**3.9**	**4.1**	**4.9**	**4.6**	**5.2**	**3.6**

The effect of dispersion on the *basic properties* of mostly small molecules is minor. The SCAN-D3 WTMAD of 6.7 kcal/mol is very good and in between the accuracy of a typical GGA and a hybrid functional. Of this subgroup, the mindless benchmark (MB08-165) consisting of artificial molecules stands out. The set has been designed to explore the breadth of chemical space and specifically analyze the DFAs far away from any training set to test their robustness.

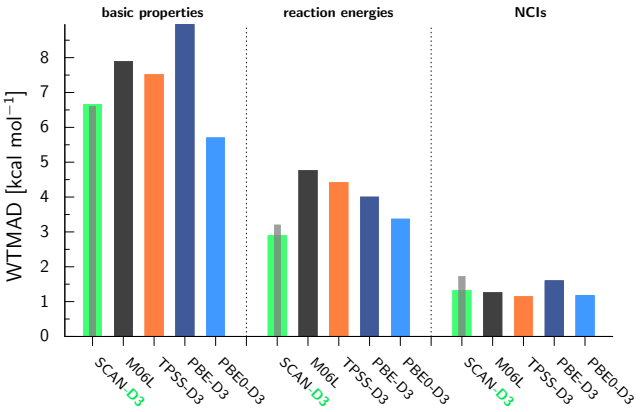

FIG. 4: Weighted mean absolute deviations (WTMADs) for the three categories (basic properties, reaction energies, and noncovalent interactions) of the large GMTKN30 database composed of 30 individual benchmarks sets given in Table IV.[28,96] For SCAN, we show both the plain functional (gray bar) and the dispersion corrected variant in order to highlight the influence of the long-range correction.

The WTMAD of SCAN-D3 for the *reaction energies* is excellent at 2.9 kcal/mol and surpases any other meta-GGA to date. Even typical hybrid functionals like PBE0-D3 and B3LYP-D3 are worse with WTMADs of 3.4 and 4.7 kcal/mol, respectively. The SCAN results for isomerization (ISO34, ISOL22) are particularly outstanding, and in the subgroup of reaction energies the D3 dispersion correction leads to only small improvements.

For the group of *noncovalent interactions* the dispersion correction has the largest impact by reducing the SCAN WTMAD from 1.7 kcal/mol to 1.3 kcal/mol. Compared to other functionals this reduction is moderate, and especially intrinsically more repulsive DFAs can reduce the WTMAD below 1 kcal/mol (e.g. revPBE-D3[97]). The most problematic systems are the water clusters in WATER27 where the plain SCAN functional already overestimates the binding energies. This is then enhanced by the attractive dispersion contribution resulting in the worst performance of the selected methods. Hao *et al.* applied the meta-GGA made simple (MGGA-MS) with a D3 correction to the GMTKN30 set and found that it delivers top-notch performance for WATER27, with an MAD below 2 kcal/mol.[98] This illustrates that it is possible to describe hydrogen bonds in water accurately via a nonempirical construction. Similar problems for water containing systems have been recognized for the PBE functional,[93] and are probably connected to an overpolarization problem in strong hydrogen bond networks related to intrinsic self-interaction error. On the other hand, SCAN-D3 is very accurate for molecular conformations with MADs below 0.5 kcal/mol for all 4 sets (PCONF, ACONF, SCONF, CYCONF).

Overall, SCAN-D3 performs very well for the GMTKN30 with a WTMAD of 3.9 kcal/mol, one of the lowest for the meta-GGA class. Interestingly, SCAN-D3 delivers superior performance compared to the M06L functional even though parts of GMTKN30 are included in the training set of the Minnesota functionals. A similar picture can be seen when comparing error statistics of molecular and atomic energies with the method of atomic equivalents. The root mean square error on 592 species are 7.5, 4.7, and 4.2 kcal/mol for LSDA, M06L, and SCAN, respectively,[99] reproducing closely the trend shown by the GMTKN30 database.

IV. CONCLUSIONS

In this work we have combined the SCAN meta-GGA with a long-range correction for London dispersion interactions. We provide default damping parameters for the D3 scheme with zero and rational damping, and VV10 dispersion corrections. The resulting SCAN-D3 method was tested on a broad set of systems with the main focus on accurate geometries, as this represents the most advantageous aspect of the meta-GGA functional class. Even considering hardware improvements, DFT will be the leading method to compute *ab initio* equilibrium structures in the foreseeable future.

The molecular geometries of SCAN-D3 exceed the accuracy of all other (meta-)GGAs thus far, while noncovalent binding energies are good (L7, X23) to very good (S22), producing high quality potential energy surfaces of molecular dimers and organic crystals. Due to the self-interaction error intrinsic in semilocal functionals, SCAN, and thus SCAN-D3, overestimates the strength of hydrogen bonds. Thermochemistry and kinetics were shown to be in excellent agreement with reference values as demonstrated on the large GMTKN30 database, resulting in a WTMAD of 3.9 kcal/mol. Overall, SCAN-D3 delivers accurate properties that are close to the results of more computationally demanding methods. Importantly, this has been achieved by a nonempirical semilocal functional. SCAN-D3 overall outperforms both the empirical M06L and the most widely used PBE-D3 functionals in about 80% of the considered test sets.

The long-range dispersion correction to SCAN is most important in systems that bind through long-range dispersion, such as the benzene crystal and the L7 set of large molecular complexes. As a consequence of the lack of structure in the long-range correction, SCAN without D3 can be reasonably good for the geometry, but not the binding energy, of even the benzene crystal.

V. COMPUTATIONAL DETAILS

For all molecular computations, we used a developer version of TURBOMOLE 7.0.[100] The M06L functional is computed via the XCfun interface.[101] We use converged single-particle basis sets of quadruple-ζ quality (def2-QZVP).[102,103] Additional diffuse functions are used for the WATER27 and G21EA benchmark sets.[104] For heavy elements these are combined with the Stuttgart-Dresden effective core potentials, that effectively include scalar relativistic effects.[105] Only some hybrid PBE0 results that have been taken from previous work were evaluated with the slightly smaller def2-TZVP basis. For the semi-local exchange-correlation part the numerical quadrature grids m4 (4 for SCAN) are used. For geometry optimizations with SCAN, the radial grid size must be substantially increased to radsize 60 or 70, see the Supporting Information. The RI-J approximation was used[106–108] with default auxiliary basis sets.[109] Standard convergence threshold for SCF convergence (10^{-7} a.u.) and tight thresholds for geometry convergence (10^{-4} a.u.) were applied. Solid state calculations were conducted with a modified VASP5.3 program suite.[110,111] To approach the single-particle basis set limit, a projector-augmented plane-wave (PAW[112,113]) basis set with a large energy cutoff of 1000 eV was applied. The PBE0 hybrid single-point energies (Figure 3 (b)) are calculated with a smaller energy cutoff of 500 eV. The Brillouin zone is sampled with dense k grids of approximately $1/40\,\text{Å}^{-1}$ generated via the Monkhorst-Pack scheme. For efficient geometry relaxations and three-body gradients of the D3 scheme in periodic boundary conditions, we use a developer version of the CRYSTAL14 program.[114]

In the current Turbomole implementation, the requirements of SCAN's exchange-correlation functional on the numerical integration grid are unusually high, leading to an increased computational cost compared to TPSS by a factor of 2 to 10. However, SCAN has decreased numerical problems in VASP, where SCAN only requires slightly denser Fourier grids compared to the PBE GGA.

We thank Stefan Grimme for helpful discussions concerning the D3 correction scheme and the importance of SCAN's numerical stability, and F. Furche for insight on the grid sensitivity in TURBOMOLE. J.G.B. acknowledges support by the Humboldt foundation within the Feodor-Lynen program. J.E.B. was supported by the U.S. Department of Energy under grant #DE-SC0010499. J.S. and J.P.P. were supported by the U.S. National Science Foundation under grant #DMR-1305135 (with support from CTMC).

* Electronic address: g.brandenburg@ucl.ac.uk

[1] R. G. Parr and W. Yang, *Density-Functional Theory of Atoms and Molecules* (Oxford University Press, Oxford, 1989).
[2] W. Kohn, Rev. Mod. Phys. **71**, 1253 (1998).
[3] U. von Barth and L. Hedin, J. Phys. C **5**, 1629 (1972).
[4] V. V. Karasiev, T. Sjostrom, J. Dufty, and S. B. Trickey, Phys. Rev. Lett. **112**, 076403 (2014).
[5] J. P. Perdew, K. Burke, and M. Ernzerhof, Phys. Rev. Lett. **77**, 3865 (1996), erratum *Phys. Rev. Lett.* **78**, 1396 (1997).
[6] A. D. Becke, Phys. Rev. A **38**, 3098 (1988).

[7] C. Lee, W. Yang, and R. G. Parr, Phys. Rev. B **37**, 785 (1988).
[8] J. Tao, J. P. Perdew, V. N. Staroverov, and G. E. Scuseria, Phys. Rev. Lett. **91**, 146401 (2003).
[9] Y. Zhao and D. G. Truhlar, J. Chem. Phys. **125**, 194101 (2006).
[10] R. Peverati and D. G. Truhlar, J. Phys. Chem. Lett. **3**, 117 (2011).
[11] R. Peverati and D. G. Truhlar, Phys. Chem. Chem. Phys. **14**, 13171 (2012).
[12] N. Mardirossian and M. Head-Gordon, J. Chem. Phys. **142**, 074111 (2015).
[13] J. M. del Campo, J. L. Gázquez, S. Trickey, and A. Vela, Chemical Physics Letters **543**, 179 (2012).
[14] J. Sun, B. Xiao, and A. Ruzsinszky, J. Chem. Phys. **137**, 051101 (2012).
[15] J. Sun, A. Ruzsinszky, and J. P. Perdew, Phys. Rev. Lett. **115**, 036402 (2015).
[16] J. Sun, R. Remsing, Y. Zhang, Z. Sun, A. Ruzsinszky, H. Peng, Z. Yang, A. Paul, U. Waghmare, X. Wu, et al., Nat. Chem. (to appear).
[17] A. D. Becke, J. Chem. Phys. **98**, 1372 (1993).
[18] S. Grimme, J. Chem. Phys. **124**, 034108 (2006).
[19] S. Grimme and M. Steinmetz, Phys. Chem. Chem. Phys. **18**, 20926 (2016).
[20] K. Hui and J.-D. Chai, J. Chem. Phys. **144**, 044114 (2016).
[21] L. A. Burns, A. Vazquez-Mayagoitia, B. G. Sumpter, and C. D. Sherrill, J. Chem. Phys. **134**, 084107 (2011).
[22] J. Klimes and A. Michaelides, J. Chem. Phys. **137**, 120901 (2012).
[23] S. Grimme, WIREs Comput. Mol. Sci. **1**, 211 (2011).
[24] S. Grimme, J. Antony, S. Ehrlich, and H. Krieg, J. Chem. Phys. **132**, 154104 (2010).
[25] O. A. Vydrov and T. Van Voorhis, J. Chem. Phys. **133**, 244103 (2010).
[26] R. Sabatini, T. Gorni, and S. de Gironcoli, Phys. Rev. B **87**, 041108 (2013).
[27] H. Peng, Z.-H. Yang, J. Sun, and J. P. Perdew, submitted to Phys. Rev. X (2016), arXiv:1510.05712.
[28] L. Goerigk and S. Grimme, J. Chem. Theory Comput. **7**, 291 (2011).
[29] S. A. Maurer, D. S. Lambrecht, J. Kussmann, and C. Ochsenfeld, J. Chem. Phys. **138**, 014101 (2013).
[30] M. Schütz, O. Masur, and D. Usvyat, J. Chem. Phys. **140**, 244107 (2014).
[31] C. Riplinger, B. Sandhoefer, A. Hansen, and F. Neese, J. Chem. Phys. **139**, 134101 (2013).
[32] J. G. Brandenburg, E. Caldeweyher, and S. Grimme, Phys. Chem. Chem. Phys. **18**, 15519 (2016).
[33] E. R. Johnson, R. A. Wolkow, and G. A. DiLabio, Chem. Phys. Lett. **394**, 334 (2004).
[34] E. R. Johnson, A. D. Becke, C. D. Sherrill, and G. A. DiLabio, J. Chem. Phys. **131**, 034111 (2009).
[35] J. P. Perdew, J. Tao, V. N. Staroverov, and G. E. Scuseria, J. Chem. Phys. **120**, 6898 (2004).
[36] S. E. Wheeler and K. N. Houk, J. Chem. Theory Comput. **6**, 395 (2010).
[37] Z.-H. Yang, H. Peng, J. Sun, and J. P. Perdew, Phys. Rev. B **93**, 205205 (2016).
[38] See supplemental material for discussion and test of SCANs numerical grid dependence and individual geometries and ingteraction energies of the discussed benchmark sets.
[39] A. Zangwill and P. Soven, Phys. Rev. A **21**, 1561 (1980).
[40] J. F. Dobson and T. Gould, J. Phys.: Condens. Matter **24**, 073201 (2012).
[41] S. Grimme, A. Hansen, J. G. Brandenburg, and C. Bannwarth, Chem. Rev. **116**, 5105 (2016).
[42] L. M. Woods, D. A. R. Dalvit, A. Tkatchenko, P. Rodriguez-Lopez, A. W. Rodriguez, and R. Podgornik, Rev. Mod. Phys. (2016), arXiv:1509.03338.
[43] O. A. Vydrov and T. Van Voorhis, J. Chem. Phys. **132**, 164113 (2010).
[44] O. A. Vydrov and T. Van Voorhis, Phys. Rev. A **81**, 062708 (2010).
[45] O. A. Vydrov and T. Van Voorhis, Phys. Rev. Lett. **104**, 099304 (2010).
[46] W. Hujo and S. Grimme, J. Chem. Theory Comput. **7**, 3866 (2011).
[47] H. B. G. Casimir and D. Polder, Phys. Rev. **73**, 360 (1948).
[48] A. Tkatchenko and M. Scheffler, Phys. Rev. Lett. **102**, 073005 (2009).
[49] A. Tkatchenko, R. A. DiStasio, R. Car, and M. Scheffler, Phys. Rev. Lett. **108**, 236402 (2012).
[50] A. D. Becke and E. R. Johnson, J. Chem. Phys. **123**, 154101 (2005).
[51] A. D. Becke and E. R. Johnson, J. Chem. Phys. **122**, 154104 (2005).
[52] A. D. Becke and E. R. Johnson, J. Chem. Phys. **124**, 014104 (2006).
[53] A. D. Becke and E. R. Johnson, J. Chem. Phys. **127**, 154108 (2007).
[54] B. M. Axilrod and E. Teller, J. Chem. Phys. **11**, 299 (1943).
[55] Y. Muto, Proc. Phys. Soc. Jpn. **17**, 629 (1943).
[56] R. A. DiStasio, V. V. Gobre, and A. Tkatchenko, J. Phys.: Condens. Matter **26**, 213202 (2014).
[57] J. F. Dobson, Int. J. Quant. Chem. **114**, 1157 (2014).
[58] M. R. Kennedy, A. R. McDonald, A. E. DePrince, M. S. Marshall, R. Podeszwa, and C. D. Sherrill, J. Chem. Phys. **140**, 121104 (2014).
[59] S. Grimme, S. Ehrlich, and L. Goerigk, J. Comput. Chem. **32**, 1456 (2011).
[60] W. Hujo and S. Grimme, J. Chem. Theory Comput. **7**, 3866 (2011).
[61] O. A. Vydrov and T. V. Voorhis, J. Chem. Theory Comput. **8**, 1 (2012).
[62] J. Moellmann and S. Grimme, J. Phys. Chem. C **118**, 7615 (2014).
[63] J. Řezáč, K. E. Riley, and P. Hobza, J. Chem. Theory Comput. **7**, 2427 (2011).
[64] B. Brauer, M. K. Kesharwani, S. Kozuch, and J. M. L. Martin, J. Chem. Theory Comput. **tba** (2016).
[65] J. Witte, M. Goldey, J. B. Neaton, and M. Head-Gordon, J. Chem. Theory Comput. **11**, 1481 (2015).
[66] S. Grimme, G. Brandenburg, C. Bannwarth, and A. Hansen, J. Chem. Phys. **143**, 054107 (2015).
[67] R. Sure, J. G. Brandenburg, and S. Grimme, ChemistryOpen **5**, 94 (2016).
[68] L. Goerigk, J. Phy. Chem. Lett. **6**, 3891 (2015).
[69] All reference values are used as given in J. Chem. Phys. 143, 054107 (2015).
[70] C. Adamo and V. Barone, J. Chem. Phys. **110**, 6158 (1999).
[71] R. Peverati and D. G. Truhlar, Phil. Trans. R. Soc. A **372**, 20120476 (2014).

[72] M. Bühl and H. Kabrede, J. Chem. Theory Comput. **2**, 1282 (2006).
[73] S. Grimme and M. Steinmetz, Phys. Chem. Chem. Phys. **15**, 16031 (2013).
[74] C. Puzzarini, M. Heckert, and J. Gauss, J. Chem. Phys. **128**, 194108 (2008).
[75] A. M. Burow, J. E. Bates, F. Furche, and H. Eshuis, J. Chem. Theory Comput. **10**, 180 (2014).
[76] T. Risthaus, M. Steinmetz, and S. Grimme, J. Comput. Chem. **35**, 1509 (2014).
[77] D. J. Lacks and R. G. Gordon, Phys. Rev. A **47**, 4681 (1993).
[78] Y. Zhang, W. Pan, and W. Yang, J. Chem. Phys. **107**, 7921 (1997).
[79] P. Jurecka, J. Sponer, J. Cerny, and P. Hobza, Phys. Chem. Chem. Phys. **8**, 1985 (2006).
[80] T. Takatani, E. G. Hohenstein, M. Malagoli, M. S. Marshall, and C. D. Sherrill, J. Chem. Phys. **132**, 144104 (2010).
[81] M. S. Marshall, L. A. Burns, and C. D. Sherrill, J. Chem. Phys. **135**, 194102 (2011).
[82] R. Sedlak, T. Janowski, M. Pitoňák, J. Řezáč, P. Pulay, and P. Hobza, J. Chem. Theory Comput. **9**, 3364 (2013).
[83] H. Kruse, A. Mladek, K. Gkionis, A. Hansen, S. Grimme, and J. Sponer, J. Chem. Theory Comput. **11**, 4972 (2015).
[84] DLPNO-CCSD(T)/CBS* with TCutPairs of 10^{-5} Eh (published elsewhere, compare with ref.[83]).
[85] K. Pernal, R. Podeszwa, K. Patkowski, and K. Szalewicz, Phys. Rev. Lett. **103**, 263201 (2009).
[86] É. D. Murray, K. Lee, and D. C. Langreth, J. Chem. Theory Comput. **5**, 2754 (2009).
[87] S. L. Price, Chem. Soc. Rev. **43**, 2098 (2014).
[88] M. A. Neumann, F. J. J. Leusen, and J. Kendrick, Angew. Chem. Int. Ed. **47**, 2427 (2008).
[89] C. C. Pantelides, C. S. Adjiman, and A. V. Kazantsev, Top Curr Chem **345**, 25 (2014).
[90] A. Otero-de-la-Roza and E. R. Johnson, J. Chem. Phys. **137**, 054103 (2012).
[91] A. M. Reilly and A. Tkatchenko, J. Chem. Phys. **139**, 024705 (2013).
[92] V. S. Bryantsev, M. S. Diallo, A. C. T. van Duin, and W. A. Goddard, J. Chem. Theory Comput. **5**, 1016 (2009).
[93] J. G. Brandenburg, T. Maas, and S. Grimme, J. Chem. Phys. **142**, 124104 (2015).
[94] J. Sun, R. C. Remsing, Y. Zhang, Z. Sun, A. Ruzsinszky, H. Peng, Z. Yang, A. Paul, U. Waghmare, X. Wu, et al. (2016), arXiv:1511,01089.
[95] L. Goerigk and S. Grimme, J. Chem. Theory Comput. **6**, 107 (2010).
[96] L. Goerigk and S. Grimme, Phys. Chem. Chem. Phys. **13**, 6670 (2011).
[97] Y. Zhang and W. Yang, Phys. Rev. Lett. **80**, 890 (1998).
[98] P. Hao, J. Sun, B. Xiao, A. Ruzsinszky, G. I. Csonka, J. Tao, S. Glindmeyer, and J. P. Perdew, J. Chem. Theory Comput. **9**, 355 (2013).
[99] J. P. Perdew, J. Sun, R. M. Martin, and B. Delley, Int. J. Quantum Chem. **116**, 847 (2016).
[100] F. Furche, R. Ahlrichs, C. Httig, W. Klopper, M. Sierka, and F. Weigend, WIREs Comput Mol Sci **4**, 91 (2014).
[101] U. Ekström, L. Visscher, R. Bast, A. J. Thorvaldsen, and K. Ruud, J. Chem. Theory Comput. **6**, 1971 (2010).
[102] F. Weigend and R. Ahlrichs, Phys. Chem. Chem. Phys. **7**, 3297 (2005).
[103] F. Weigend, F. Furche, and R. Ahlrichs, J. Chem. Phys. **119**, 12753 (2003).
[104] R. A. Kendall, T. H. Dunning, and R. J. Harrison, J. Chem. Phys. **96**, 6796 (1992).
[105] K. A. Peterson, D. Figgen, E. Goll, H. Stoll, and M. Dolg, J. Chem. Phys. **119**, 11113 (2003).
[106] E. J. Baerends, D. E. Ellis, and P. Ros, Chem. Phys. **2**, 41 (1973).
[107] B. I. Dunlap, W. D. Connolly, and J. R. Sabin, J. Chem. Phys. **71**, 3396 (1979).
[108] K. Eichkorn, O. Treutler, H. Öhm, M. Häser, and R. Ahlrichs, Chem. Phys. Lett. **240**, 283 (1995).
[109] F. Weigend, Phys. Chem. Chem. Phys. **8**, 1057 (2006).
[110] G. Kresse and J. Hafner, Phys. Rev. B **47**, 558 (1993).
[111] G. Kresse and J. Furthmüller, J. Comp. Mat. Sci. **6**, 15 (1996).
[112] P. E. Blöchl, Phys. Rev. B **50**, 17953 (1994).
[113] G. Kresse and J. Joubert, Phys. Rev. B **59**, 1758 (1999).
[114] R. Dovesi, R. Orlando, A. Erba, C. M. Zicovich-Wilson, B. Civalleri, S. Casassa, L. Maschio, M. Ferrabone, M. De La Pierre, P. D'Arco, et al., Int. J. Quantum Chem. **114**, 1287 (2014).